Effect of Sintering on Magnetic Properties of $Ni_{0.55}Zn_{0.45}Fe_2O_4$

Manoj M. Kothawale, R. B. Tangsali, G. K. Naik & J. S. Budkuley

Journal of Superconductivity and Novel Magnetism
Incorporating Novel Magnetism

ISSN 1557-1939
Volume 26
Number 11

J Supercond Nov Magn (2013)
26:3293-3298
DOI 10.1007/s10948-013-2171-y

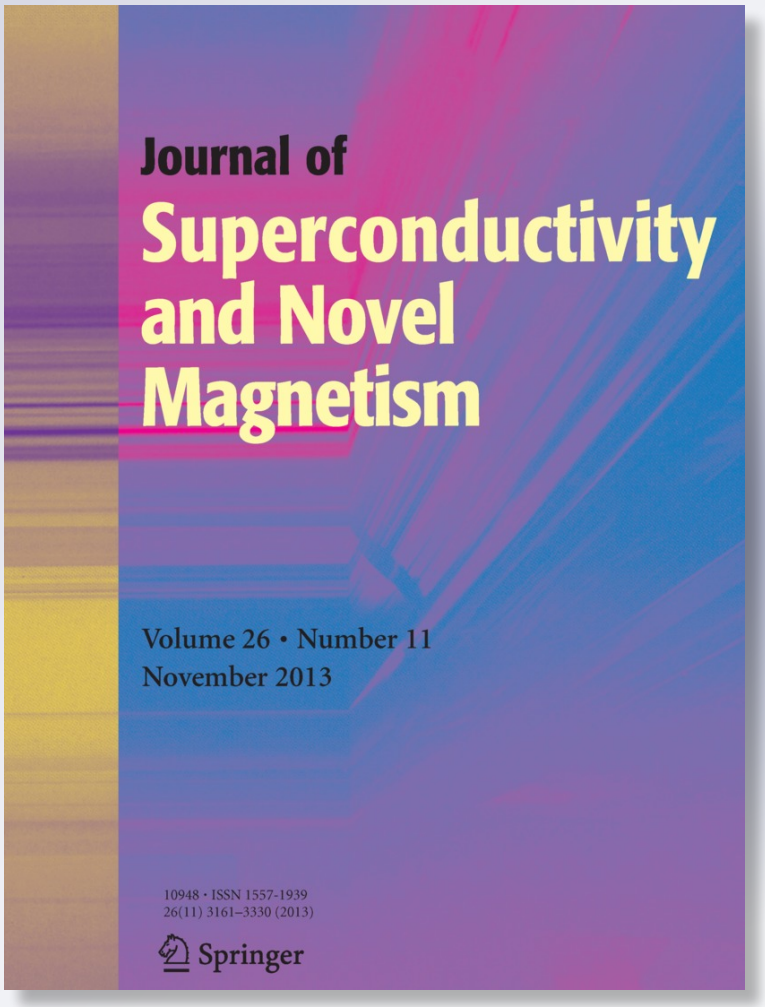

Springer

J Supercond Nov Magn (2013) 26:3293–3298
DOI 10.1007/s10948-013-2171-y

ORIGINAL PAPER

Effect of Sintering on Magnetic Properties of $Ni_{0.55}Zn_{0.45}Fe_2O_4$

Manoj M. Kothawale · R.B. Tangsali · G.K. Naik · J.S. Budkuley

Received: 16 January 2013 / Accepted: 13 March 2013 / Published online: 12 April 2013

Abstract Bulk $Ni_{0.55}Zn_{0.45}Fe_2O_4$ samples were obtained by sintering their nanopowder at 1100 °C, 1200 °C, and 1300 °C. Improvement in crystallinity on sintering was identified from increase in intensity of the XRD peaks and grain development in SEM micrographs. Saturation magnetization increased from 81.7 emu/g to 85.3 emu/g as the sintering temperature increased from 1100 °C to 1300 °C. Initial permeability increases whereas the relative loss factor, resonance frequency, and DC resistivity decreases with increasing the sintering temperature. Curie temperatures obtained from low field AC normalized susceptibility and permeability measurements are in good agreement. The DC resistivity of the samples in the present case is two orders higher than the reported values of samples prepared using conventional ceramic method.

Keywords Ni–Zn ferrites · XRD · SEM · Initial permeability · Dc resistivity · Curie temperature

M.M. Kothawale (✉)
Department of Physics, D.M.S. College of Arts Science and Commerce, Assagao, Goa 403 507, India
e-mail: manojkothawale@yahoo.com

R.B. Tangsali
Department of Physics, Goa University, Taleigao Plateau, Goa 403 206, India
e-mail: rbtangsali@unigoa.ac.in

G.K. Naik
Department of Chemistry, S.P. C. College of Arts and Science, Margao, Goa, India

J.S. Budkuley
Department of Chemistry, Goa University, Taleigao Plateau, Goa 403 206, India

1 Introduction

Ferrites cover high potential for several electromagnetic devices in the radio frequency region, as they have frequency dependent properties such as permeability [1, 2]. The value of initial permeability gives you an indication of how easily a given material can be magnetized. One of the main considerations of high frequency performance of ferrites is high eddy current losses, which prevent interaction of the magnetic field with ferrite component, produces heat, and spoils the device performance [3]. These losses can be reduced by having a material with high resistivity. Owing to miniaturization of electronic devices more efforts are being made to develop material operating in MHz region showing low power losses. Properties of ferrites are known to be sensitive to processing techniques, compositions, microstructures, heat treatments, etc. [4]. Study of thermal variations of initial permeability of polycrystalline ferrites can be used as a quality test in preparation of ferrite samples [5]. This paper focuses on effect of a sintering temperature on saturation magnetization, Curie temperature, initial permeability, and relative loss factor of $Ni_{0.55}Zn_{0.45}Fe_2O_4$.

2 Experimental

Nanoparticles of $Ni_{0.55}Zn_{0.45}Fe_2O_4$ were synthesized using microwave assisted combustion method as reported in our previous paper Kothawale et al. [6]. The fine nanopowder of this sample was pressed into pellets (10 mm dia and 2 mm thick) and toroids (inner and outer dia of 10 mm and 20 mm, respectively, and height of 0.34 mm) by applying pressure of 75 kN for 5 min. The pallets and toroids were then sintered in a programmable furnace at 1100 °C, 1200 °C, and 1300 °C in air for 4 h by maintaining heating and cooling

rate as 5 °C min^{-1}. The X-ray powder diffraction patterns were recorded on Rigaku X-ray diffractometer using Cu-K_α radiation and 2θ scanning range from 20° to 80°. Saturation magnetization, coercivity, and retentivity temperature were measured at room temperature using automated high field Hysteresis loop tracer. Low field AC susceptibility measurements in the temperature range of 300 K to 800 K were carried out using Likhite's automated double coil set up. The SEM images were obtained from Joel Model JSM (6360) (SEM). A winding of 100 turns of superenameled doubly insulated copper wire of gauge 33 were made on each toroid to carry out initial permeability measurements. Inductance values were recorded at room temperature within a frequency variation of 0.1 MHz to 3 MHz using Wayne Kerr 6440B precision component analyzer setup. Inductance and loss measurements were also carried out for selected frequencies within temperature range of 30 °C to 500 °C. Bulk densities were measured using Archimedes principle [7]. DC resistivities at room temperature were measured by a two-probe method using Keithley electrometer. The pellets of bulk samples were coated with silver on both surfaces for good electrical contact with the probe while measuring DC resistivity.

3 Results and Discussion

3.1 XRD Analysis

The X-ray diffraction (XRD) patterns of the bulk samples at sintering temperatures of 1100 °C, 1200 °C, and 1300 °C are shown in Fig. 1. The absence of unwanted impurity peaks in XRD spectra and peaks positions confirm that samples have a single phase cubic spinel structure and single phase purity is not affected on sintering [8]. The increase in sharpness and intensity of peaks with increasing the sintering temperature is an indication of improvement in crystallinity of the samples. The inset of Fig. 1 shows shifting of peaks toward higher Bragg's angle with the increase in sintering temperature. This shifting of peak positions indicates lattice contraction of the sample with increasing sintering temperature.

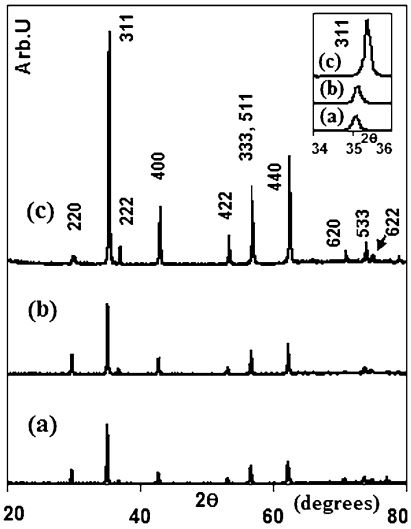

Fig. 1 XRD patterns of $Ni_{0.55}Zn_{0.45}Fe_2O_4$ samples sintered at (**a**) 1100 °C, (**b**) 1200 °C, and (**c**) 1300 °C. *Inset* shows shifting of (311) peaks with sintering temperature

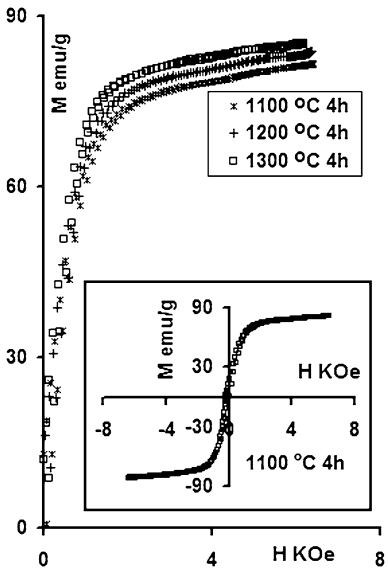

Fig. 2 Variation of magnetization of $Ni_{0.55}Zn_{0.45}Fe_2O_4$ samples with a static magnetic field (*Inset* shows the $M-H$ loop of the sample sintered at 1100 °C)

3.2 Magnetic Properties

3.2.1 Magnetization

The variations of magnetization with static magnetic field (up to 7 kOe) of samples are shown in Fig. 2. (Inset shows $M-H$ loop of sample sintered at 1100 °C.) The hysteresis loop is deviated from rectangularity, and hence illustrates magnetic behavior of soft ferrite [6]. It can be seen that magnetization increases with the field and attains near saturation above 6 kOe. The values of saturation magnetization (M_s), coercivity (H_c), and retentivity (M_r) are given in Table 1. The values of M_s obtained in the present work are higher than reported for conventionally prepared ferrites [9, 10]. This high M_s is attributed to the method of preparation. The M_s increases with an increase in the sintering temperature. This is attributed mainly due to increase in grain sizes [11], as seen from scanning electron microscope (SEM) images in Fig. 3. The reduction of coercivity (H_c) by about 30 % for sample sintered at 1300 °C compared to

Table 1 Various parameters of $Ni_{0.55}Zn_{0.45}Fe_2O_4$ samples: saturation magnetization (M_s), retentivity (M_r), Coercivity (H_c), Curie temperature (T_c^a and T_c^b) from ac susceptibility and initial permeability measurements, respectively, resonance frequency (F_r), room temperature initial permeability at resonance (μ_i^r), relative loss factor at resonance (RLF_r), bulk density (ρ_B), and room temperature DC resistivity (ρ_{RT})

Parameters	Sample sintered at		
	1100 °C	1200 °C	1300 °C
M_s emu/g	81.7	83.8	85.3
M_r emu/g	55.8	29.6	37.1
H_c Oe	81.9	105.1	70.6
T_c^a °C	275 ± 10	260 ± 10	300 ± 10
T_c^b °C	280	255	290
F_r MHz	>3	2.34	1.90
μ_i^r	1965	6334	65524
RLF_r	1.6×10^{-3}	9.9×10^{-4}	5.8×10^{-4}
ρ_B g/cm^3	4.59	4.88	4.84
ρ_{RT} Ω cm	5.1×10^7	4.8×10^7	3.2×10^7

at 1200 °C, can be attributed to an increase in grain sizes. Larger grains tend to consist of greater number of domain walls, and hence, contribution of wall movement to magnetization or demagnetization is greater than that of domain rotation.

The magnetization/demagnetization caused by domain wall movement requires less energy than that required by domain rotation [12]. Minimum retentivity of 29.6 emu/g was found for sample obtained at a sintering temperature of 1200 °C.

The Scanning Electron Microscope (SEM) images of the samples sintered at temperature of 1100 °C, 1200 °C, and 1300 °C are shown in Fig. 3. It can be seen that the grains and grain boundaries are not clearly visible at sintering temperature of 1100 °C (Fig. 3(a)). At this sintering temperature, SEM micrograph could not resolve the images of grains, and hence, histogram of grain size distribution of the same is not presented in this paper. The compact microstructure with well crystallites having bigger sizes and less pores can be observed at sintering temperature of 1200 °C (Fig. 3(b)) and 1300 °C (Fig. 3(c)). For comparison purposes, we have presented SEM images at all the sintering temperatures with fixed magnification of 5000. The decrease in intergranular pores can be noticed at sintering temperature of 1300 °C. The histograms of grain size distribution for sample sintered at 1200 °C and 1300 °C are shown in Fig. 4. It was found that, minimum and maximum grain sizes were of 0.9 μm and 4.8 μm for sample sintered at 1200 °C, whereas, 2.8 μm and 7.3 μm for 1300 °C. The maximum in the histogram was found in the range of 2 μm for sample sintered at 1200 °C; whereas, the same was found at 5 μm for 1300 °C sample.

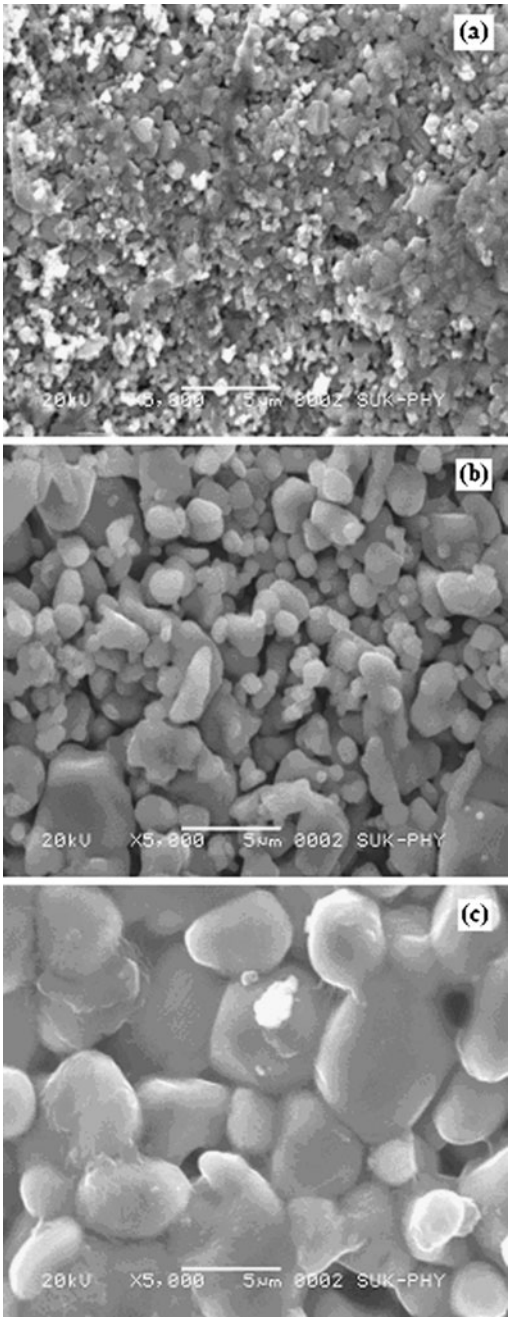

Fig. 3 SEM micrographs of $Ni_{0.55}Zn_{0.45}Fe_2O_4$ samples sintered at (**a**) 1100 °C, (**b**) 1200 °C and (**c**) 1300 °C

3.2.2 *Ac Susceptibility*

Thermal variations of normalized susceptibility for samples are shown in Fig. 5, and corresponding Curie temperatures are recorded in Table 1. These curves reflect that, all the samples are showing a multidomain (MD) structure.

The Curie temperature of ferrites generally decreases with increasing sintering temperature. However, in present case, sample sintered at 1300 °C shows higher T_c compared

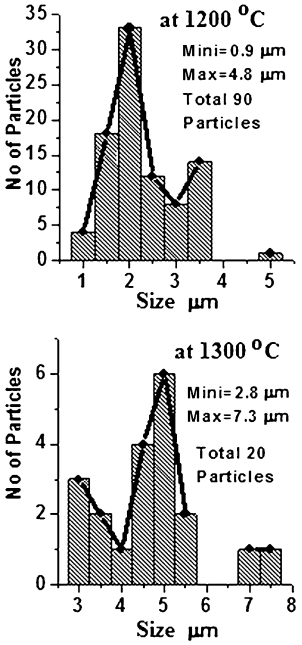

Fig. 4 Histogram of grain size distribution obtained from SEM micrographs of $Ni_{0.55}Zn_{0.45}Fe_2O_4$ samples sintered at 1200 °C and 1300 °C

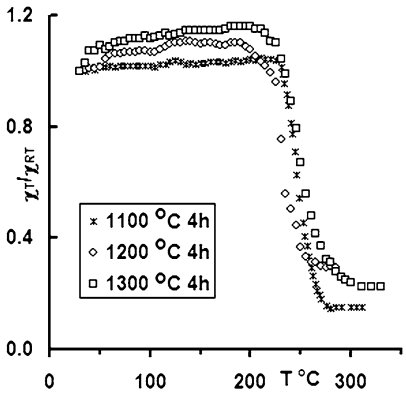

Fig. 5 Variation of normalized susceptibility with temperature for $Ni_{0.55}Zn_{0.45}Fe_2O_4$

to other two samples. This may be attributed to decrease in distance between magnetic moments of A and B sites, due to a decrease in lattice parameter, which is confirmed by shifting of XRD peaks toward a higher Bragg's angle for sample sintered at 1300 °C. For lower lattice, parameter A–B interaction increases due to an increase in the overlapping of the orbital of Fe_A^{3+}–O^{2-}–Fe_B^{3+} linkages [12]. Higher T_c observed at sintering temperature of 1300 °C may also be due to its observed higher grain growth and low porosity (see Fig. 3(c)), which helps Zn^{2+} ions to change spin ordering from Y-K to Neel's type, and energy required to offset the antiparallel spin is more than canted Y-K type [11, 13]. This increase may partly be attributed to zinc volatilization at higher sintering temperature leading to increase in the Fe/Ni ratio [13].

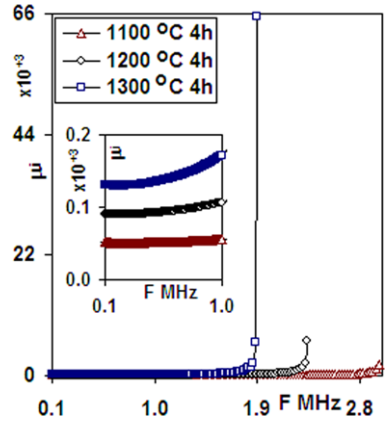

Fig. 6 Initial permeability as a function of frequency for $Ni_{0.55}Zn_{0.45}Fe_2O_4$ (*inset* shows variation of permeability up to 1 MHz)

3.2.3 *Initial Permeability and Relative Loss Factor*

For high performance, ferrite material needs high initial permeability (μ_i), high DC resistivity, and low power loss. High μ_i is associated with uniform grain size, less anisotropy, low porosity, and high density, which in turn depends on method of preparation and sintering conditions [14]. The initial permeability (μ_i) was calculated using Eq. (1).

$$\mu_i = \frac{2\pi L}{N^2 h \ln(\frac{OD}{ID})\mu_o} \tag{1}$$

where L is inductance in Henry, N is the number of turns of copper wire on toroid, h is height of core in meters, OD and ID is outer and inner diameter of toroid in meters, and μ_o is permeability of free space (1.25×10^{-6} H m^{-1}). The variation of initial permeability as a function of frequency (0.1 to 3 MHz) is shown in Fig. 6 (Inset shows μ_i up to 1 MHz).

It is observed that, μ_i remains almost independent below resonance frequency for all the samples. Values obtained below resonance frequency are approximately 55, 107, and 172 for samples sintered at 1100 °C, 1200 °C, and 1300 °C, respectively. These values are higher than reported by Aktar Hussain et al. [13] for similar sintering temperatures. The observed increase in permeability with sintering temperature is due to significant contribution of domain walls, as grain sizes and density increases on sintering [3]. These increases may be also due to an increase in saturation magnetization, decrease in anisotropy, and low porosity on sintering [15]. The maximum permeability of the ample sintered at 1300 °C is attributed to its larger grain growth with less non-magnetic voids or pores. It is observed that the higher the μ_i, lower the resonance frequency. This agrees with Snoek's limit $f_r\mu_i^r$ = constant, where f_r is resonance frequency and μ_i^r is the permeability value at resonance. Thus, there is always a compromise between high frequency and

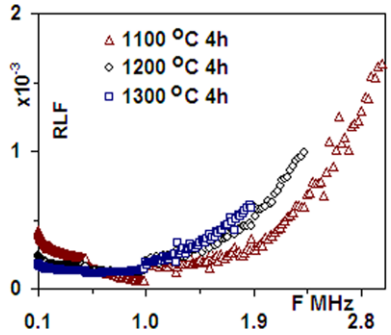

Fig. 7 Variation of Relative loss factor as a function of frequency for $Ni_{0.55}Zn_{0.45}Fe_2O_4$

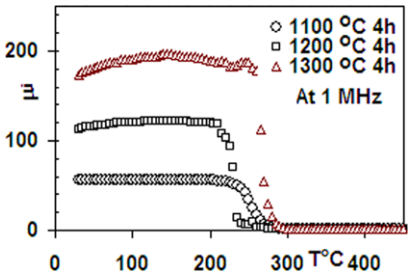

Fig. 8 Variation of initial permeability with temperature at frequency of 1 MHz for $Ni_{0.55}Zn_{0.45}Fe_2O_4$

high permeability. Normally, two resonance peaks are observed in ferrites: one at lower frequency ∼10–100 MHz, which is due to the domain wall oscillations and the other at higher frequencies ∼few GHz due to Larmor precession of electron spins [16]. The observed resonance peak in the present work is indicative of domain wall oscillations or resonance [17]. The resonance frequencies and corresponding permeability values are given in Table 1. The shift of f_r from above 3 MHz to 1.90 MHz was observed as sintering increases from 1100 °C to 1300 °C. For sample obtained at sintering temperature of 1100 °C, resonance peak may be beyond a measurable frequency limit (3 MHz) of our apparatus. The main reason for this is their small grain sizes. The SEM images have clearly shown the smaller grain sizes at sintering temperature of 1100 °C. The magnetic loss is measured in the form of a relative loss factor (RLF). RLF is calculated as ratio of $\tan\delta/\mu_I$, and its variation with frequency is shown in Fig. 7. The RLF increases with increase in frequency until resonance. The RLF values at resonance are given in Table 1.

Variations of initial permeability with temperature at 1 MHz frequency are shown in Fig. 8. It is observed that for 1300 °C sample, initial permeability increases very slowly with temperature, reaches peak value, and drops gradually to zero at Curie temperature. The maxima in initial permeability correspond to the point of zero anisotropy fields [15]. However, for sample sintered at 1100 °C and 1200 °C, initial permeability remains almost constant initially with increase

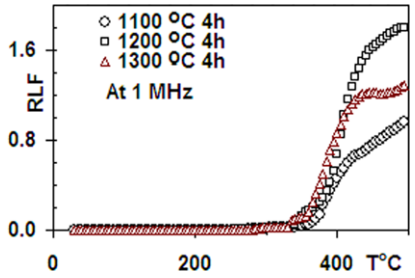

Fig. 9 Variation of relative loss factor with temperature at frequency of 1 MHz for $Ni_{0.55}Zn_{0.45}Fe_2O_4$

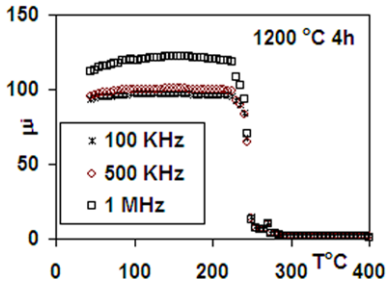

Fig. 10 Variation of initial permeability with temperature at three fixed frequencies for sample sintered at 1200 °C

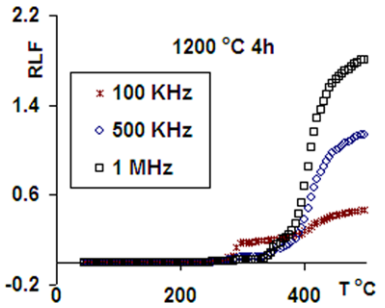

Fig. 11 Variation of RLF with temperature at three fixed frequencies for sample sintered at 1200 °C

in temperature and drops gradually to zero at Curie temperature. Curie temperatures obtained via this method are given in Table 1; they closely match with those obtained using low field AC susceptibility technique. The sharpness in the drop of initial permeability at the Curie point is a measure of homogeneity in the composition of sample [17]. Further optimization in the preparation and sintering profile can be tried to improve the homogeneity. RLF versus temperature at frequency of 1 MHz is shown in Fig. 9. The RLF values remain almost constant at lower temperature and starts increasing above Curie temperature, as the system become disorder beyond T_c.

The temperature variations of permeability and RLF at three fixed frequencies (100 kHz, 500 kHz, and 1 MHz) for sample sintered at 1200 °C are shown in Figs. 10 and 11, respectively. Similar patterns of variations can be seen at all

the three frequencies. The maximum density of 4.88 g/cm^3 was found for sample sintered at 1200 °C. The values of DC at room temperature are given in Table 1. These values are greater than reported for the standard ceramic method as well as by sol-gel method [3, 18]. High resistivity is an indication of negligible bulk eddy current loss. For comparison, sample prepared via standard ceramic and sol-gel method having composition $Ni_{0.30}Zn_{0.70}Fe_2O_4$ sintered for 4 h at 1250 °C in air shows resistivity of 1.8×10^4 Ω cm and 4.5×10^5 Ω cm, respectively; whereas in present work it is 4.8×10^7 Ω cm (1200 °C) and 3.2×10^7 Ω cm (1300 °C) for $Ni_{0.55}Zn_{0.45}Fe_2O_4$. This higher value of resistivity may be attributed to method of sample preparation and sintering parameters.

4 Conclusions

The sample shows lattice contraction with increase in the sintering temperature, and the lattice constant reduced from 8.4029 Å (at 1100 °C) to 8.3956 Å (at 1300 °C). Saturation magnetization and bulk density increases with sintering temperature; whereas the room temperature DC resistivity decreases. SEM micrograph showed better grain growth and clear grain boundaries for sample sintered at a temperature of 1300 °C. The highest Curie temperature is found for sample sintered at 1300 °C. Resonance frequency shifts to lower value, whereas permeability increases with sintering temperature. Higher permeability with increasing sintering temperature is attributed to increase in grain sizes. Samples showed low loss and high permeability in the measured frequency range of 0.1 MHz to 3 MHz, and hence, stand promising in medium frequency applications. Further optimization in preparation and sintering conditions can be undertaken to improve compromise between higher working frequency and required permeability.

References

1. Nakamura, T.: J. Appl. Phys. **88**, 348–353 (2000)
2. Hiti, E.M.A.: J. Magn. Magn. Mater. **164**, 187–196 (1996)
3. Zahi, S., Hashim, M., Daud, A.R.: J. Magn. Magn. Mater. **308**, 177–182 (2007)
4. Mahmud, S.T., Akther Hossain, A.K.M., Abdul Hakim, A.K.M., Seki, M., Kawai, T., Tabata, H.: J. Magn. Magn. Mater. **305**, 269–274 (2006)
5. Cedillo, E., Ocampo, J., Rivera, V., Valenzuela, R.: J. Phys. E, Sci. Instrum. **13**, 383–386 (1980)
6. Kothawale, M.M., Tangsali, R.B., Naik, G.K., Budkuley, J.S.: J. Supercond. Nov. Magn. **25**, 1907–1911 (2012)
7. Sheikh, A.D., Mathe, V.L.: J. Mater. Sci. **43**, 2018–2025 (2008)
8. Jadhav, S.S., Shirsath, S.E., Toksha, B.G., Shukla, S.J., Jadhav, K.M.: Chin. J. Chem. Phys. **21**, 381–386 (2008)
9. Verma, A., Goel, T.C., Mendiratta, R.G., Kishan, P.: J. Magn. Magn. Mater. **208**, 13–19 (2000)
10. Srinivasan, T.T., Ravindranathan, P., Cross, L.E., Roy, R., Newnham, R.E.: J. Appl. Phys. **63**(8), 3789–3793 (1988)
11. Matsuo, Y., Mochizuki, T., Ishikura, M., Sakaki, I.: J. Magn. Soc. Jpn. **20**, 429–432 (1996)
12. Costa, A.C.F.M., Tortella, E., Morelli, M.R., Kiminami, R.H.G.A.: J. Magn. Magn. Mater. **256**, 174–182 (2003)
13. Akther Hossain, A.K.M., Mahmud, S.T., Abdul Hakim, A.K.M., Seki, M., Kawai, T., Tabata, H.: J. Magn. Magn. Mater. **305**, 210–219 (2007)
14. Keluskar, S.H., Tangsali, R.B., Naik, G.K., Budkuley, J.S.: J. Magn. Magn. Mater. **305**, 296–303 (2006)
15. Zahi, S., Daud, A.R., Hashim, M.: J. Mater. Chem. Phys. **106**, 452–456 (2007)
16. Singh, A.K., Goel, T.C., Mendiratta, R.G., Thakur, O.P., Prakash, C.: J. Appl. Phys. **92**(7), 3872–3876 (2002)
17. Mathur, P., Thakur, A., Singh, M.: J. Phys. Chem. Solids **69**, 187–192 (2008)
18. Su, H., Zhang, H., Xiang, X., Tang: J. Magn. Magn. Mater. **283**, 157–160 (2004)